J|A|C|S ARTICLES

Published on Web 05/18/2010

Shutting Down Secondary Reaction Pathways: The Essential Role of the Pyrrolyl Ligand in Improving Silica Supported d^0-ML_4 Alkene Metathesis Catalysts from DFT Calculations

Xavier Solans-Monfort,[†] Christophe Copéret,*[,‡] and Odile Eisenstein*[,§]

Departament de Química, Universitat Autònoma de Barcelona, E-08173 Bellaterra, Spain, Université de Lyon, Institut de Chimie de Lyon, C2P2 UMR5265 (CNRS−CPE−Université Lyon 1), ESCPE Lyon, F-308 - 43 Boulevard du 11 Novembre 1918 F-69616 Villeurbanne Cedex, France, and Institut Charles Gerhardt, Université Montpellier 2, CNRS 5253, cc 1501, Place Eugène Bataillon, F-34095 Montpellier, France

Received February 24, 2010; E-mail: coperet@cpe.fr; odile.eisenstein@univ-montp2.fr

Abstract: The efficiency of silica supported d^0 ML_4 alkene metathesis catalysts [(≡SiO)M(NR^1)(=CHR^2)(X)] (M = Mo, W; R^1 = aryl and alkyl) is influenced by the nature of the X ancillary ligand. Replacing the alkyl ligand by a pyrrolyl ligand dramatically increases the performance of the catalyst. DFT calculations on the metathesis, the deactivation, and the byproduct formation pathways for the imido Mo and W and the alkylidyne Re complexes give a rational for the role of pyrrolyl ligand. Dissymmetry at the metal center leads to more efficient catalyst even when the difference in σ-donating ability between X and OSi is not large. β-H transfer at the square based pyramid metallacyclobutane is the key step for catalyst deactivation and byproduct formation. Overall, the greatest benefit of substituting the ancillary alkyl by a pyrrolyl ligand, [(≡SiO)M(ER^1)(=CHR^2)(pyrrolyl)], is in fact not to improve the efficiency of the catalytic cycle of alkene metathesis, but to shut down deactivation and byproduct formation pathways. Pyrrolyl ligand, and more generally ligands having metal-bound-atoms more electronegative than carbon, disfavor mostly the two first steps (β-H transfer at the metallacyclobutane and subsequent insertion of an ethene in the M−H bond) of the deactivation channel. The [(≡SiO)M(ER^1)(=CHR^2)(pyrrolyl)] catalyst is thus highly efficient because pyrrolyl ligand is optimal: (i) it is still a better electron donor than the siloxy group, thus, favoring the metathesis pathway (dissymmetry at the metal center); and (ii) the nitrogen of the pyrrolyl ligand is more electronegative than the carbon of the alkyl group, thus, specifically disfavoring the decomposition of the metallacyclobutane intermediate via β-H transfer.

Introduction

Alkene metathesis has become a key reaction in the chemical industry and in academia. While the petrochemical industry has used this technology for 40 years, it has gained even more importance in the recent years with the increasing world demand of propene. The production of this compound can indeed be augmented through the ethenolysis of the C_4 cut (butenes) in the presence of WO_3-based heterogeneous catalysts (Lummus process).[1] Recent advances in homogeneous catalysis have shown that alkene metathesis could also be used to synthesize more complex substrates containing functional groups, including pharmaceuticals.[2] It has also been proposed to use this technology to convert unsaturated fatty esters into α-olefin.[3] These advances have been possible through the development of molecular catalysts through structure−reactivity relationship, based on the knowledge that metallocarbenes and metallacyclobutanes are key reaction intermediates.[4] While these species have been isolated under homogeneous conditions and tuned over the years,[5] they remain elusive in heterogeneous catalysts. This is probably one of the reasons why it has been so difficult to avoid a more empirical approach to improve heterogeneous alkene metathesis catalysts. This has led to undertake a research effort toward the design and the preparation of supported alkene metathesis catalysts with a well-defined coordination sphere in order to combine the advantages of homogeneous and heterogeneous catalysis.[6] It has only been recently that the first fully characterized well-defined supported alkylidene systems have appeared.[7] In particular, the silica supported Re-based catalyst, [(≡SiO)Re(≡C*t*Bu)(=CH*t*Bu)(CH$_2$*t*Bu)],[7b−d] displayed un-

[†] Universitat Autònoma de Barcelona.
[‡] Institut de Chimie de Lyon.
[§] Université Montpellier 2.

(1) Mol, J. C. *J. Mol. Catal. A: Chem.* **2004**, *213*, 39–45.
(2) (a) Connon, S. J.; Blechert, S. *Angew. Chem., Int. Ed.* **2003**, *42*, 1900–1923. (b) Hoveyda, A. H.; Schrock, R. R. *Comprehensive Asymmetric Catalysis Supplement 1*; Jacobsen, E. N.; Pfaltz, A.; Yamamoto, H., Eds.; Springer: Berlin, Germany, 2004; pp 207−233. (c) Hoveyda, A. H.; Malcolmson, S. J.; Meek, S. J.; Zhugralin, A. R. *Angew. Chem., Int. Ed.* **2010**, *49*, 34–44.
(3) Mol, J. C. *Top. Catal.* **2004**, *27*, 97–104.
(4) (a) Hérisson, J. L.; Chauvin, Y. *Makromol. Chem.* **1971**, *141*, 161–76. (b) Chauvin, Y. *Angew. Chem., Int. Ed.* **2006**, *45*, 3741–3747.
(5) (a) Grubbs, R. H. *Angew. Chem., Int. Ed.* **2006**, *45*, 3760–3765. (b) Schrock, R. R. *Angew. Chem., Int. Ed.* **2006**, *45*, 3748–3759.
(6) (a) Ballard, D. G. H. *Adv. Catal.* **1973**, *23*, 263–325. (b) Ballard, D. G. H. *Coord. Polym.* **1975**, 223–262. (c) Yermakov, Y. I.; Kuznetsov, B. N.; Zakharov, V. A. *Stud. Surf. Sci. Catal.* **1981**, *8*, 1. (d) Basset, J. M.; Choplin, A. *J. Mol. Catal.* **1983**, *21*, 95–108. (e) Copéret, C.; Chabanas, M.; Petroff Saint-Arroman, R.; Basset, J.-M. *Angew. Chem., Int. Ed.* **2003**, *42*, 156–181.

 10.1021/ja101597s

Table 1. Catalytic Performances of a Series of Well-Defined Silica Supported Alkylidene Complexes

	catalyst precursors (≡SiO)(X)(M≡ER¹)(═CHR²) with R² = *t*Bu or CMe_2Ph		catalyst performances			
entry	M≡ER¹	X	TOF[a]	TON[b]	Selectivity[c]	reference
1	Re≡C*t*Bu	CH_2*t*Bu	120	6000	96.0%	7b,8
2	Mo≡NAr[d]	CH_2*t*Bu	120	22000	99.4%	12
3	W≡NAr[d]	CH_2*t*Bu	8.4	6000	99.4%	13
4	Mo≡NAr[d]	Pyrrolyl	362	62000	>99.9%	16
5	Mo≡NAr[d]	2,5-MePyrrolyl	320	101000	>99.9%	16
6	Mo≡NAd[e]	2,5-MePyrrolyl	780	275000	>99.9%	16
7	W≡NAr[d]	2,5-MePyrrolyl	24	25000	>99.9%	17

[a] Initial activity (after 5 min) expressed in mol of propene converted per min and per mol of M. [b] Cumulated turnover numbers after 1500 min. [c] Selectivity in 2-butenes of butenes. [d] Ar = 2,6-diisopropylphenyl. [e] Ad = Adamantyl.

precedented high activity in propene metathesis at low temperatures (Table 1, Entry 1) and converted functionalized alkenes without the need of co-catalysts (as usually required with heterogeneous catalysts),[8a] but it also showed a relatively fast deactivation (1st order in ethene) and the unexpected formation of 1-butene as a primary product.[8b] These unexpected results were investigated through DFT calculations, which showed that alkene metathesis was a four-elementary step reaction involving coordination of the alkene, [2 + 2]-cycloaddition to generate the metallacyclobutanes and the corresponding reverse steps.[9] These computational studies also showed that high activity of this catalyst originated from the dissymmetry at the metal center, that is, the presence of a strong (alkyl) and a weak (siloxy) σ-donor ligands, which induced low energy barriers for coordination as well as a decrease stability of the metallacyclobutane intermediates (*vide infra*). Earlier theoretical studies of alkene metathesis by d^0 metal catalysts have addressed other mechanistic aspects of the reaction.[10] Additionally, deactivation and byproduct formation were investigated by DFT calculations in combination with kinetic and *in situ* spectroscopic studies on the Re-based silica supported catalyst showing that these two processes originate primarily from β-H transfer at the metallacyclobutane intermediates having a SBP geometry followed by ethene insertion and subsequent H-transfer steps.[8b] These combined experimental and computational investigations as well as the advances in preparative methods for [M(≡NAr)(═CH*t*Bu)(CH_2*t*Bu)$_2$][11] resulted in the development of the corresponding isoelectronic silica supported group 6 imido alkyl alkylidene complexes, [(≡SiO)M(≡NAr)(═CH*t*Bu)(CH_2*t*Bu)] (M = Mo[12] and W,[13] Table 1, Entries 2 and 3 respectively), which showed improved performances in term of TON and 2-butene selectivity. More recently, the development of bis-amido[14] and in particular bis-pyrrolyl[15] complexes has allowed the access to [(≡SiO)M(≡NAr)(═CH*t*Bu)(NR_2)] (M = Mo[16] and W[17]), where the ancillary neopentyl ligand is replaced by the corresponding amido group; this has translated into greatly improved catalytic performances (Table 1, Entries 4−7), both in terms of higher TON (up to ca. 300 000) and selectivity (<0.1% of 1-butene if any).[18] Note that the corresponding isoelectronic molecular monopyrrolyl complexes (MAP) have also been developed, and they also display unprecedented activities.[19]

In view of our current knowledge on the origin of the activity, selectivity and stability of the silica supported Re-based alkyl systems and of the greatly improved performances in term of activity, TON and selectivity of the corresponding silica supported Mo and W systems having an ancillary pyrrolyl in place of a neopentyl ligand, we use DFT calculations to investigate the origins of the remarkable role of the pyrrolyl ligand in these silica supported Mo- and W-based alkene

(7) (a) Chabanas, M.; Quadrelli, E. A.; Fenet, B.; Copéret, C.; Thivolle-Cazat, J.; Basset, J.-M.; Lesage, A.; Emsley, L. *Angew. Chem., Int. Ed.* **2001**, *40*, 4493–4496. (b) Chabanas, M.; Baudouin, A.; Copéret, C.; Basset, J. M. *J. Am. Chem. Soc.* **2001**, *123*, 2062–2063. (c) Lesage, A.; Emsley, L.; Chabanas, M.; Copéret, C.; Basset, J.-M. *Angew. Chem., Int. Ed.* **2002**, *41*, 4535–4538. (d) Chabanas, M.; Baudouin, A.; Copéret, C.; Basset, J.-M.; Lukens, W.; Lesage, A.; Hediger, S.; Emsley, L. *J. Am. Chem. Soc.* **2003**, *125*, 492–504. (e) Le Roux, E.; Chabanas, M.; Baudouin, A.; de Mallmann, A.; Copéret, C.; Quadrelli, E. A.; Thivolle-Cazat, J.; Basset, J.-M.; Lukens, W.; Lesage, A.; Emsley, L.; Sunley, G. J. *J. Am. Chem. Soc.* **2004**, *126*, 13391–13399.

(8) (a) Chabanas, M.; Copéret, C.; Basset, J.-M. *Chem.—Eur. J.* **2003**, *9*, 971–975. (b) Leduc, A.-M.; Salameh, A.; Soulivong, D.; Chabanas, M.; Basset, J.-M.; Copéret, C.; Solans-Monfort, X.; Clot, E.; Eisenstein, O.; Böhm, V. P. W.; Röper, M. *J. Am. Chem. Soc.* **2008**, *130*, 6288–6297.

(9) (a) Solans-Monfort, X.; Clot, E.; Copéret, C.; Eisenstein, O. *J. Am. Chem. Soc.* **2005**, *127*, 14015–14025. (b) Poater, A.; Solans-Monfort, X.; Clot, E.; Copéret, C.; Eisenstein, O. *J. Am. Chem. Soc.* **2007**, *129*, 8207–8216.

(10) (a) Rappé, A. K.; Goddard, W. A., III. *J. Am. Chem. Soc.* **1980**, *102*, 5114–5115. (b) Folga, E.; Ziegler, T. *Organometallics* **1993**, *12*, 325–337. (c) Fox, H. H.; Schofield, M. H.; Schrock, R. R. *Organometallics* **1994**, *13*, 2804–2815. (d) Wu, Y.-D.; Peng, Z.-H. *J. Am. Chem. Soc.* **1997**, *119*, 8043–8049. (e) Wu, Y.-D.; Peng, Z.-H. *Inorg. Chim. Acta* **2003**, *345*, 241–254. (f) Monteyne, K.; Ziegler, T. *Organometallics* **1998**, *17*, 5901–5907. (g) Goumans, T. P. M.; Ehlers, A. W.; Lammertsma, K. *Organometallics* **2005**, *24*, 3200–3206. (h) Handzlik, J.; Ogonowski, J. *J. Mol. Catal. A: Chem.* **2001**, *175*, 215–225. (i) Handzlik, J. *J. Catal.* **2003**, *220*, 23–34. (j) Handzlik, J.; Sautet, P. *J. Catal.* **2008**, *256*, 1–14.

(11) (a) Sinha, A.; Schrock, R. R. *Organometallics* **2004**, *23*, 1643–1645. (b) Lopez, L. P. H.; Schrock, R. R. *J. Am. Chem. Soc.* **2004**, *126*, 9526–9527.

(12) (a) Blanc, F.; Copéret, C.; Thivolle-Cazat, J.; Basset, J.-M.; Lesage, A.; Emsley, L.; Sinha, A.; Schrock, R. R. *Angew. Chem., Int. Ed.* **2006**, *45*, 1216–1220. (b) Blanc, F.; Salameh, A.; Thivolle-Cazat, J.; Basset, J.-M.; Copéret, C.; Sinha, A.; Schrock, R. R. *C. R. Chim.* **2008**, *11*, 137–146.

(13) Rhers, B.; Salameh, A.; Baudouin, A.; Quadrelli, E. A.; Taoufik, M.; Copéret, C.; Lefebvre, F.; Basset, J.-M.; Solans-Monfort, X.; Eisenstein, O.; Lukens, W. W.; Lopez, L. P. H.; Sinha, A.; Schrock, R. R. *Organometallics* **2006**, *25*, 3554–3557.

(14) Sinha, A.; Schrock, R. R.; Müller, P.; Hoveyda, A. H. *Organometallics* **2006**, *25*, 4621–4626.

(15) Hock, A. S.; Schrock, R. R.; Hoveyda, A. H. *J. Am. Chem. Soc.* **2006**, *128*, 16373–16375.

(16) (a) Blanc, F.; Thivolle-Cazat, J.; Basset, J.-M.; Copéret, C.; Hock, A. S.; Tonzetich, Z. J.; Schrock, R. R. *J. Am. Chem. Soc.* **2007**, *129*, 1044–1045. (b) Blanc, F.; Berthoud, R.; Salameh, A.; Basset, J.-M.; Copéret, C.; Singh, R.; Schrock, R. R. *J. Am. Chem. Soc.* **2007**, *129*, 8434–8435.

(17) Blanc, F.; Berthoud, R.; Copéret, C.; Lesage, A.; Emsley, L.; Singh, R.; Kreickmann, T.; Schrock, R. R. *Proc. Nat. Acad. Sci. U.S.A.* **2008**, *105*, 12123–12127.

(18) Copéret, C. *Dalton Trans.* **2007**, 5498–5504.

(19) (a) Singh, R.; Schrock, R. R.; Müller, P.; Hoveyda, A. H. *J. Am. Chem. Soc.* **2007**, *129*, 12654–12655. (b) Wampler, K. M.; Schrock, R. R.; Hock, A. S. *Organometallics* **2007**, *26*, 6674–6680. (c) Malcolmson, S. J.; Meek, S. J.; Sattely, E. S.; Schrock, R. R.; Hoveyda, A. H. *Nature* **2008**, *456*, 933–937. (d) Ibrahem, I.; Yu, M.; Schrock, R. R.; Hoveyda, A. H. *J. Am. Chem. Soc.* **2009**, *131*, 3844–3845. (e) Lee, Y. J.; Schrock, R. R.; Hoveyda, A. H. *J. Am. Chem. Soc.* **2009**, *131*, 10652–10661. (f) Marinescu, S. C.; Schrock, R. R.; Li, B.; Hoveyda, A. H. *J. Am. Chem. Soc.* **2009**, *131*, 58–59. (g) Sattely, E. S.; Meek, S. J.; Malcolmson, S. J.; Schrock, R. R.; Hoveyda, A. H. *J. Am. Chem. Soc.* **2009**, *131*, 943–953.

Scheme 1

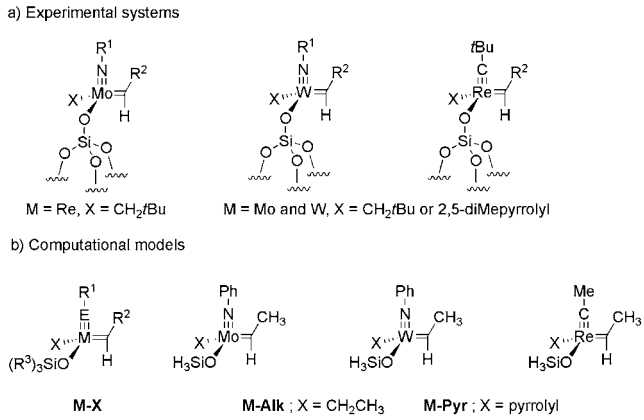

metathesis catalysts, including the Re-based catalysts, which are currently not known.

Computational Details

Calculations have been carried out with the hybrid B3PW91 density functional,[20] as implemented in the Gaussian03 package[21] on the model systems M(≡NPh)(═CHCH$_3$)(X)(OSiH$_3$) (M = Mo or W) and Re(≡CCH$_3$)(═CHCH$_3$)(X)(OSiH$_3$) with X = CH$_2$CH$_3$ for **M-Alk** or X = pyrrolyl for **M-Pyr** (Scheme 1). The Mo, W, Re, and Si atoms have been represented with the quasi relativistic effective core pseudopotentials (RECP) of the Stuttgart group and the associated basis sets augmented with a polarization function.[22] The remaining atoms (C, H, N, and O) have been represented with 6-31G(d,p) basis sets.[23] The B3PW91 geometry optimizations were performed without any symmetry constraints, and the nature of the extrema (local minima or transition states) was checked by analytical frequency calculations. In addition, when needed, the connection between transition state, reactant, and product was verified by an intrinsic reaction coordinates (IRC) calculation. The discussion of the results is based on the electronic energies *E* without any zero point energy (ZPE) corrections because inclusion of the ZPE corrections does not significantly modify the results.

Results

The role of the pyrrolyl versus alkyl ligand in silica supported d^0 tetra-coordinated group 6−7 alkylidene metathesis catalysts was investigated by comparing first, their structures; second, their reactivity in alkene metathesis (reaction pathways using ethene as a model substrate);[9] and third, their deactivation pathways initiated by β-H transfer, whose importance was established for the silica supported Re alkyl alkylidene system.[8b]

Models. The DFT calculations were carried out on molecular model systems M(≡ER^1)(═CHR^2)(X)(OSiR$^3_3$) (**M-X**) with **M**(≡ER^1) = **Mo**(≡NPh), **W**(≡NPh), and **Re**(≡CCH$_3$), R^2 = CH$_3$, X = CH$_2$CH$_3$ (**Alk**) or pyrrolyl (**Pyr**) and R^3 = H (Scheme 1). M(≡NPh) was used as model of the experimental arylamido Mo and W systems (ER^1 = NR^1 with R^1 = 2,6-diisopropylphenyl), Re(≡CCH$_3$) as model of Re(≡C*t*Bu), ═CHMe as model of the alkylidene ligand, X = CH$_2$CH$_3$ as model of the neopentyl group (CH$_2$*t*Bu), X = pyrrolyl as model for the parent and the 2,5-dimethylpyrrolyl, and OSiH$_3$ as model for the silica surface.[24]

Scheme 2

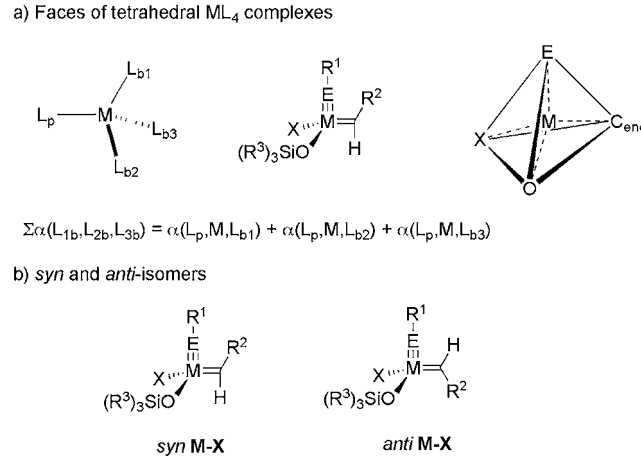

Structures of the Catalysts. The structure of the pyrrolyl complexes **M-Pyr** shares common structural features with **M-Alk**: **Mo-Alk**,[25] **W-Alk**,[25] and **Re-Alk**.[26] In particular, all **M-Pyr** complexes display a pseudotetrahedral geometry (Table S1), in which ER^1, the metal, the alkylidene C$_{ene}$, and the substituent on the alkylidene group (Me) are coplanar and where the E−M−C$_{ene}$ angle is smaller (97−104°) than that expected for a tetrahedron (see Supporting Information for a more detailed presentation of specific structural features). Note also that the presence of four different ligands results in a tetrahedron with four *nonequivalent* faces (Scheme 2a and Table S1).[27] Each face of the tetrahedron is defined by three "basal" ligands (L$_{bi}$ with i = 1, 2 and 3) as L$_{b1}$, L$_{b2}$, and L$_{b3}$ and excludes the fourth "pivotal" ligand (L$_p$). For ideal tetrahedrons, the sum of the three L$_p$−M−L$_{bi}$ angles ($\sum\alpha_{Lb1,Lb2,Lb3}$) is 328.4°; a smaller value indicates a more open face; conversely, a larger value characterizes a less open face. In all cases, the least open face corresponds to [C$_{ene}$,E,X] (siloxy as pivotal ligand), while the most open one is the [X,O,E] face for **M-Pyr** (alkylidene as pivotal ligand) and the [O,E,C$_{ene}$] face for the **M-Alk** complexes (X = alkyl as pivotal ligand). It thus appears that the most open face opposes the strongest σ-donor pivotal ligand (alkyl for **M-Alk** and alkylidene for **M-Pyr**), and conversely, the least open face opposes the weakest σ-donor pivotal ligand (siloxy). For **Re-Alk**, where X, E, and C$_{ene}$ are all strong carbon based σ-donor ligands, the faces opposed to these ligands display similar opening.

All **M-Pyr** exist as two different alkylidene isomers: the *syn* isomer (alkylidene methyl group pointing toward the E−R^1

(20) (a) Perdew, J. P.; Chevary, J. A.; Vosko, S. H.; Jackson, K. A.; Pederson, M. R.; Singh, D. J.; Fiolhais, C. *Phys. Rev. B* **1992**, *46*, 6671–6687. (b) Becke, A. D. *J. Chem. Phys.* **1993**, *98*, 5648–5652.
(21) Frisch, M. J.; et al. *Gaussian03, Revision C.02*; Gaussian Inc.: Wallingford, CT, 2004.
(22) (a) Andrae, D.; Haüssermann, U.; Dolg, M.; Stoll, H.; Preuss, H. *Theo. Chim. Acta* **1990**, *77*, 123–141. (b) Bergner, A.; Dolg, M.; Küchle, W.; Stoll, H.; Preuss, H. *Mol. Phys.* **1993**, *80*, 1431–1441. (c) Ehlers, A. W.; Böhme, M.; Dapprich, S.; Gobbi, A.; Höllwarth, A.; Jonas, V.; Köhler, K. F.; Stegmann, R.; Veldkamp, A.; Frenking, G. *Chem. Phys. Lett.* **1993**, *208*, 111–114. (d) Höllwarth, A.; Böhme, M.; Dapprich, S.; Ehlers, A. W.; Gobbi, A.; Jonas, V.; Köhler, K. F.; Stegmann, R.; Veldkamp, A.; Frenking, G. *Chem. Phys. Lett.* **1993**, *208*, 237–240.
(23) Hehre, W. J.; Ditchfield, R.; Pople, J. A. *J. Chem. Phys.* **1972**, *56*, 2257–2261.
(24) Solans-Monfort, X.; Filhol, J.-S.; Copéret, C.; Eisenstein, O. *New J. Chem.* **2006**, *30*, 842–850.
(25) Poater, A.; Solans-Monfort, X.; Clot, E.; Copéret, C.; Eisenstein, O. *Dalton Trans.* **2006**, 3077–3087.
(26) Solans-Monfort, X.; Clot, E.; Copéret, C.; Eisenstein, O. *Organometallics* **2005**, *24*, 1586–1597.
(27) Schrock, R. R.; Crowe, W. E.; Bazan, G. C.; DiMare, M.; O'Regan, M. B.; Schofield, M. H. *Organometallics* **1991**, *10*, 1832–1843.

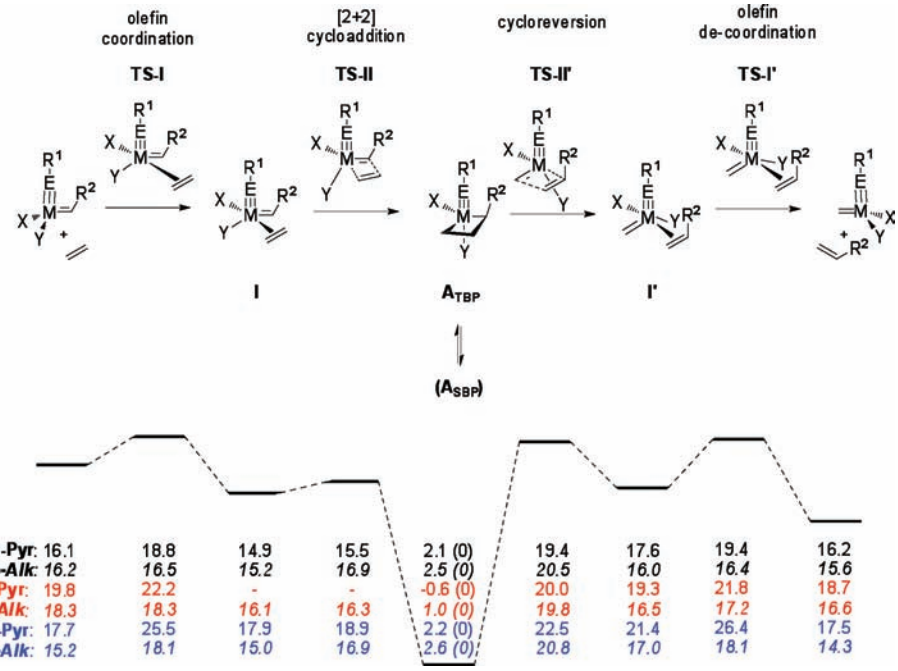

Figure 1. Alkene metathesis pathway (formation and decomposition of the TBP metallacyclobutanes): energies of intermediates and transition states in kcal mol^{-1} with respect to A_{SBP} (Y = $OSiH_3$, R^1 = Ph, R^2 = CH_3). The sign "-" indicates extrema which were not located.

Table 2. Ethene Coordination to **M-X**[a]

parameters		Mo-Pyr-TS-I	Mo-Alk-TS-I	W-Pyr-TS-I	W-Alk-TS-I	Re-Pyr-TS-I	Re-Alk-TS-I
				Energy			
$TS_{trans\ X}$		2.7	0.3	2.4	<0.1	7.8	2.9
$TS_{trans\ O}$		9.2	15.4	8.1	13.8	14.6	24.2
TS_{transE}		19.7	19.8	15.1	16.9	31.0	30.0
				Structural Parameters[b] for $TS_{trans\ X}$			
	d(M−C_2H_4)	3.378	3.444	3.368	3.487	3.283	3.354
	$\Sigma\alpha_M$	348.4	353.6	347.8	352.2	348.8	353.3
X,E,C_{ene}	α(O−M−X)	101.7	98.6	101.9	99.5	101.2	99.5
	α(E−M−X)	101.9	97.9	102.2	98.9	99.0	97.3
	α(C_{ene}−M−X)	99.5	98.0	99.9	98.9	103.1	98.3
	$\Sigma\alpha_{O,E,C}$	303.0	294.5	304.0	297.3	303.3	295.1
	$\Sigma\alpha_N$	359.6	−	359.4	−	359.9	−

[a] Transition state energies in kcal mol^{-1}, with respect to separated reactants, for coordination *trans* to X, siloxy and ER^1 and structural parameters for $TS_{trans\text{-}X}$. [b] Structural parameters for $TS_{trans\ E}$ and $TS_{trans\ O}$ are in Tables S3 and S4, respectively. Distances and angles are given in Å and degree, respectively.

ligand) with an agostic C_{ene}−H is ca. 2 kcal mol^{-1} more stable than the *anti* isomer (alkylidene methyl group pointing away from the ER^1 ligand) having no agostic interaction (Scheme 2b). These isomers can interconvert via rotation around the M−C_{ene} bond, but such process is calculated to have a relatively high energy barrier, the value being higher for X = Pyr and/or Re: 16.8 and 21.4 kcal mol^{-1} for **Mo-X** and **W-X** and 29.7−36.1 kcal mol^{-1} for **Re-X** (for further details, see Tables S1−S2 and comments in Supporting Information).

Metathesis Reaction Pathways. As previously found for **M-Alk**, the metathesis pathway involves four elementary steps for **M-Pyr**: alkene coordination, [2 + 2]-cycloaddition to metallacyclobutane intermediates, cycloreversion, and alkene decoordination (Figure 1).[9] The two last steps are essentially mirror images of the two first steps, since they only differ by the nature of coordinated alkene (ethene vs propene) and the alkylidene (ethylidene vs methylidene). The whole reaction pathway has been discussed in details previously.[9b] Here, we focus on the change resulting from replacing an alkyl by a pyrrolyl ligand on the elementary steps of alkene metathesis.

Alkene Coordination. To form the metallacycle intermediate, the alkene needs to coordinate *cis* to the alkylidene ligands. This precludes the approach toward the [O,E,X] face *trans* to the C_{ene} ligand even if it is to the most open face in the case of **M-Pyr**. This leaves three alternative approaches: *trans* to E, [X,O,C_{ene}] face, *trans* to X, [O,E,C_{ene}] face, and *trans* to O, [C_{ene},E,X] face. In all cases, the energetically preferred approach is *trans* to X (pyrrolyl or alkyl), followed by *trans* to O (siloxy); the less favored one being *trans* to E (imido or alkylidyne). At the transition state with the approach *trans* to the E ligand ($TS_{trans\text{-}E}$), the alkylidene has rotated by an angle of 50−77° from its orientation in **M-X** (Table S3). It has been mentioned above that the rotation of the alkylidene ligand has a relatively high rotational barrier, which contributes to the high energy of $TS_{trans\text{-}E}$.

Of the two productive approaches (Figure 1, Table 2 and Table S4), the transition states associated with ethene coordinating *trans* to the pyrrolyl ligand are systematically and significantly lower in energy (2.7, 2.4, and 7.8 kcal mol^{-1} for **Mo-Pyr**, **W-Pyr**, and **Re-Pyr** above separated reagents, respectively)

than these *trans* to the siloxy ligand (9.2, 8.1, and 14.6 kcal mol^{-1} for **Mo-Pyr**, **W-Pyr**, and **Re-Pyr**, respectively). This is similar to what was found for **M-Alk** complexes with a preferred approach of the alkene *trans* to the alkyl X ligand. Note that the transition state energies ($TS_{trans\text{-}X}$) are slightly lower for X = alkyl than for X = pyrrolyl (0.3, <0.1 and 2.9 kcal mol^{-1} for **Mo-Alk**, **W-Alk**, and **Re-Alk**), while the transition state energies associated with the approaches *trans* to the siloxy ligands ($TS_{trans\text{-}O}$) are higher for **M-Alk** than for **M-Pyr**. This can be understood by considering the interaction between the alkene and the metal fragment at the transition state. In all cases, the alkene is located at more than 3.0 Å from the metal center at the transition state, and thus interacts only weakly with the metal fragment. Therefore, the energy of the transition states is essentially the energy needed for distorting the metal fragment from its ground state geometry to this at the transition state (Table S5). This corresponds to the opening of a face of the tetrahedron toward a trigonal pyramid.[9] Of the two possible faces leading to productive coordination, the [O,E,C_{ene}] face, opposed to the stronger σ-donor ligand (X vs siloxy and alkyl vs pyrrolyl), is more easily opened. Noteworthy, it also corresponds to the more open of the two faces in the isolated catalyst, [O,E,C_{ene}] versus [X,E,C_{ene}], and it shows that the ligands around the metal predistort the coordination sphere toward the transition state for alkene coordination and thus prepare the metal center for the reaction. These results are general for all metals, but differences in energy between various approaches are exacerbated for **Re-X** because of the presence of the stronger σ-donating alkylidyne compared to the imido ligand in the basal plane.

The lowest energy transition states connect to alkene complexes (**M−X−I**) with the exception of **W-Pyr**, for which this complex has not been located as a minimum. The **M−X−I** complexes have a trigonal bipyramid geometry with apical X and alkene ligands and an energy close to that of separated reactants (−2.2 to +0.2 kcal mol^{-1}).

Metallacyclobutane Intermediates. From the alkene adduct, the energy barrier for [2 + 2]-cycloaddition is always very small (<2 kcal mol^{-1}), and the transition state is connected to a stable metallacyclobutane intermediate having a trigonal bipyramidal geometry, $\mathbf{A_{TBP}}$ (Table S6). For all systems, the metallacyclobutane is planar, $\Omega(M-C_\alpha-C_\beta-C_{\alpha'}) \approx 0°$, with two short $M-C_\alpha$ bonds (2.04−2.08 Å) at two basal sites of the TBP. The $M-C_\beta$ distance is also short in all cases (2.32−2.42 Å), while the two $C_\alpha-C_\beta$ bonds are always longer than those expected for a single C−C bond (1.574−1.616 Å). The third basal site is occupied by X, the stronger σ-donor ancillary ligand, that is, pyrrolyl or alkyl versus siloxy. The ER^1 and the siloxy groups occupy the apical sites. For **M-Pyr** metallacyclobutanes, the pyrrolyl is planar and perpendicular to the basal plane. The calculated structural features and notably the pyrrolyl orientation, the bond distances, and the angles in the metallacycle are in good agreement with experimental data on isoelectronic Mo and W phenoxy complexes.[28] The reaction energy is only moderately influenced by the X-ligand and is slightly greater for X = Pyr than for X = Alk (−14.0 vs −13.7 kcal mol^{-1}; −20.4 vs −17.3 kcal mol^{-1} and −15.5 vs −12.6 kcal mol^{-1} for Mo, W, and Re, respectively). This is consistent with the lower σ-donating ability of the pyrrolyl ligand, compared to the alkyl ligand.

A square-based pyramid (SBP) metallacyclobutane isomer $\mathbf{A_{SBP}}$ has also been located as a minimum, and it is slightly more stable than the TBP isomer by ca. 2 kcal mol^{-1}, with the exception of **W-X** where the difference in energy is smaller and even marginally in favor of the TBP isomer for **W-Pyr** (Figure 2 and Table S6). The geometries of the SBP and TBP metallacyclobutane complexes differ in many aspects: the SBP metallacyclobutane is folded [$\Omega(M-C_\alpha-C_\beta-C_{\alpha'}) \approx 23.6-28.1°$], it has longer $M-C_\alpha$ (2.15−2.23 Å) and $M-C_\beta$ (2.78−2.81 Å) distances but shorter $C_\alpha-C_\beta$ distances (1.515−1.525 Å). These structural features are similar to these calculated for X = Alk and are in good agreement with the characterized W-based SBP metallacyclobutane intermediates.[29] It is noteworthy that the position of the ER^1 group relative to the metallacycle, as evaluated by the $\alpha(E-M-C_\alpha)$ and $\alpha(E-M-C_{\alpha'})$ angles is similar in the TBP and SBP metallacyclobutanes, while X and siloxy ligands occupy different positions. Furthermore, for the imido **Mo−X** and **W−X** complexes, $\alpha(M-E-R^1)$ is up to 10° smaller in the SBP complex. Finally, the pyrrolyl ligand is rotated relative to the M−E bond in the SBP and not in the TBP [$\Omega(C_{Pyr}-N-M-E)$ = ca. 40 and ca. 4° for SBP and TBP, respectively]. As found for the TBP isomer, the reaction energy (SBP vs separated reactants) is affected by the metal center: tungsten SBP metallacyclobutane intermediates are about 2−3 kcal mol^{-1} lower in energy than Mo and Re metallacyclobutanes with respect to separated reagents. This reaction energy is only moderately influenced by the X-ligand, and typically slightly more negative for X = Pyr at the exception of Mo, where **Mo-Pyr-A_{SBP}** and **Mo-Alk-A_{SBP}** metallacycles are isoenergetic.

Moreover, while TBP and SBP isomers are close in energy (0.6−2.6 kcal mol^{-1}), the energy barriers for TBP−SBP interconversion are relatively high (11.9−19.8 kcal mol^{-1}), higher for X = Alk than for X = Pyr and not found for **Re-Alk**. The transition state geometries for TBP−SBP interconversion display salient features (Figure 2 and Table S7): a puckered metallacyclobutane similar to this found in the SBP isomer, an angle of 95−100° between the M−E bond and the $C_\alpha-M-C_{\alpha'}$ plane as found in both the SBP and the TBP isomers, the X ligand almost *trans* to C_α and an E−M−O angle of 120−130° compared to 180° in the TBP. Therefore, this interconversion corresponds to a turnstile process by which two ligands (X and siloxy) change position relative to the three other ones (E, C_α and $C_{\alpha'}$).[30] This is consistent with the current understanding that a turnstile mechanism applies preferentially to a Berry pseudorotation when polydentate ligands (here the metallacycle) introduce constraints.[30a,c]

Cycloreversion and Decoordination Steps. From the metallacyclobutane intermediates to the products, cycloreversion and alkene decoordination have transition states and intermediates, which are similar to those obtained for the formation of the metallacyclobutanes. The small differences are associated with the change of the alkylidene (ethylidene to methylidene) and alkene (ethene to propene) fragment.

(28) (a) Marinescu, S. C.; Schrock, R. R.; Müller, P.; Hoveyda, A. H. *J. Am. Chem. Soc.* **2009**, *131*, 10840–10841. (b) Flook, M. M.; Jiang, A. J.; Schrock, R. R.; Müller, P.; Hoveyda, A. H. *J. Am. Chem. Soc.* **2009**, *131*, 7962–7963. (c) Jiang, A. J.; Simpson, J. H.; Müller, P.; Schrock, R. R. *J. Am. Chem. Soc.* **2009**, *131*, 7770–7780.

(29) (a) Feldman, J.; Davis, W. M.; Thomas, J. K.; Schrock, R. R. *Organometallics* **1990**, *9*, 2535–2548. (b) Feldman, J.; Schrock, R. R. *Prog. Inorg. Chem.* **1991**, *39*, 1–74.

(30) (a) Ugi, I.; Marquarding, D.; Klusacek, H.; Gillespie, P.; Ramirez, F. *Acc. Chem. Res.* **1971**, *4*, 288–296. (b) Schinzel, S.; Chermette, H.; Copéret, C.; Basset, J.-M. *J. Am. Chem. Soc.* **2008**, *130*, 7984–7987. (c) Couzijn, E. P. A.; van den Engel, D. W. F.; Slootweg, J. C.; de Kanter, F. J. J.; Ehlers, A. W.; Schakel, M.; Lammertsma, K. *J. Am. Chem. Soc.* **2009**, *131*, 3741–3751.

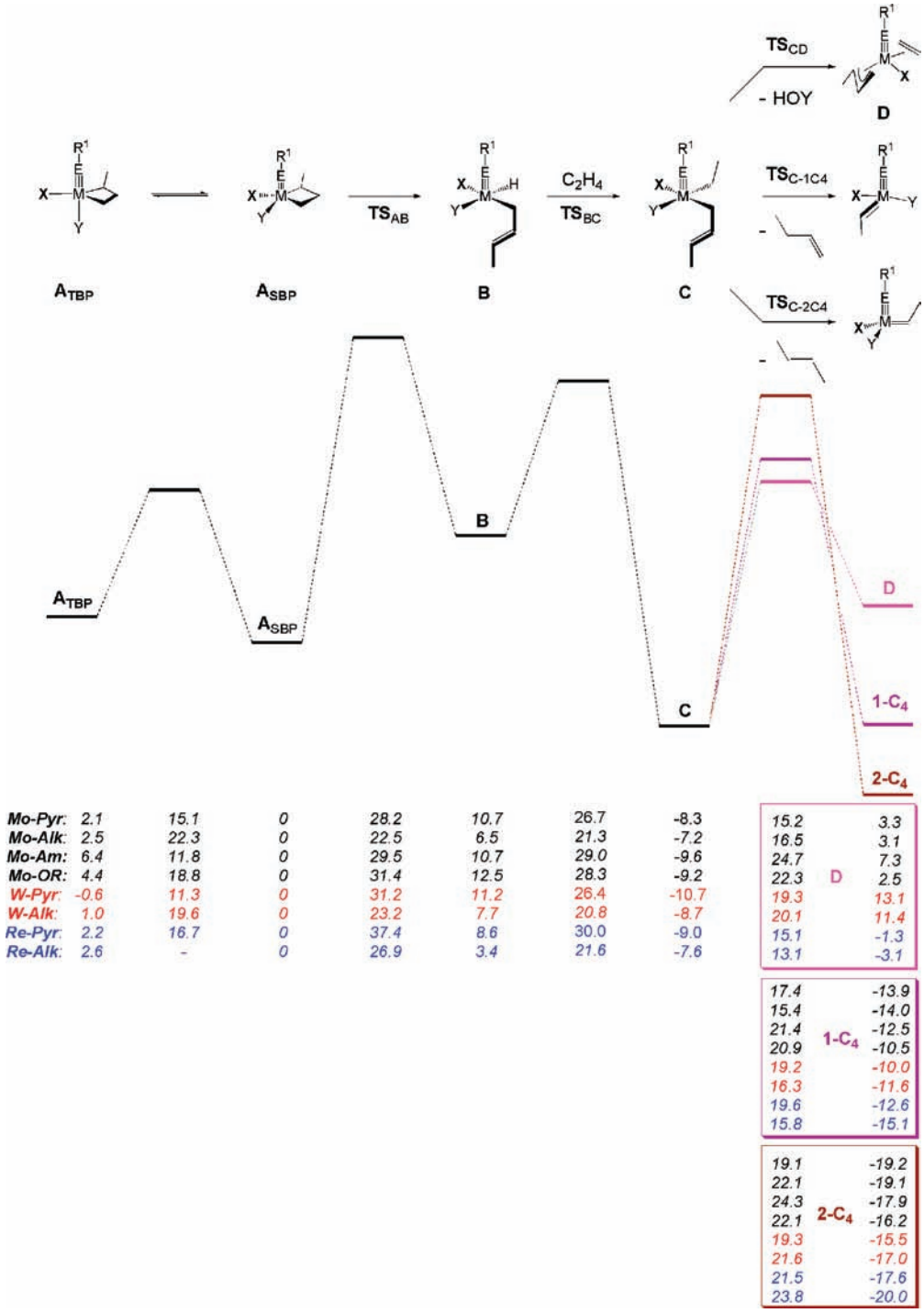

Figure 2. Formation and decomposition of the SBP metallacyclobutanes from $\mathbf{A_{TBP}}$: energies of intermediates and transition states in kcal mol^{-1} with respect to A_{SBP} (Y = $OSiH_3$, R^1 = Ph, R^2 = CH_3). The sign "-" indicates a transition state which was not located. In **Mo**−**Am**, the X ligand is NMe_2 and in **Mo**−**OR** the X ligand is OCH_3.

Deactivation and Byproduct Formation Pathways. We have recently shown by a combination of experimental and computational studies that the β-H transfer at the SBP metallacyclobutane, which has an empty coordination site, is the key step for catalyst deactivation and byproduct formation in alkene metathesis catalyzed by the silica supported rhenium complex [(≡SiO)Re(≡C*t*Bu)(═CH*t*Bu)(CH_2*t*Bu)] modeled by **Re-Alk**. This step is followed by insertion of ethene in the metal-hydride bond and further decomposition of the thus formed intermediate via intramolecular H-abstraction processes leading to degrafting (deactivation) or regeneration of the catalysts and byproduct formation (Figure 2 and Tables S8 and S9).[8] Here, we explore the influence of the metal and the X ligand (**M-X**) on the same elementary steps as previously identified for **Re-Alk** and validated for all M−X complexes (*vide supra*). Calculations show that the metal and the X ligand influence significantly the first two steps, that is, β-H transfer and ethene insertion, while subsequent steps leading to degrafting or byproduct formation are less affected.

***β*-H Transfer.** The β-H transfer step can occur either *trans* to ER^1, *trans* to the siloxy ligand or *trans* to X (alkyl or pyrrolyl). β-H transfer *trans* to the weaker σ-donor siloxy ligand is in general the energetically most favored pathway for all **M-X** systems, the only exception being for **Re-Pyr** where the β-H transfer *trans* to the pyrrolyl ligand is slightly more favorable. In all systems, this step leads to the formation of σ-bonded 2-butenyl hydride SBP complex **B**. The most stable isomer descends from the lowest energy transition state where the β-H transfer from the β-C of the metallacyclobutane occurs *trans* to the siloxy. It has a basal hydride *trans* to the siloxy group and a vacant site *trans* to the apical ER^1 group. For all **M-Pyr**, this elementary step is endoenergetic (8.6−11.2 kcal mol^{-1}) and has a high energy transition state (28.2−37.4 kcal mol^{-1} above the SBP isomer), which is 9.2−14.9 kcal mol^{-1} above the highest-energy transition state of the metathesis pathways. In contrast, for all **M-Alk** species, this elementary step is slightly less endoenergetic (3.4−7.7 kcal mol^{-1}) and more importantly is associated with a significantly lower energy transition state (22.5−26.9 kcal mol^{-1} above the SBP isomer), which thus lies only 2.0−6.1 kcal mol^{-1} above the highest-energy transition state of the metathesis pathways. As a consequence, the pyrrolyl ligand increases the energy differences between the desired alkene metathesis channel and the key step for unwanted catalyst deactivation and byproduct formation (β-H transfer).[8b] Overall, the undesired β-H transfer competes with the desired elementary steps of alkene metathesis only for **M-Alk**.

Insertion in the M−H Bond. The insertion of ethene in the metal hydride bond occurs without prior coordination to the metal center *trans* to ER^1 ligand, leading to a SBP ethyl complex **C** with apical ER^1 group. For **M-Pyr**, this process is highly exoenergetic (−19.0, −21.9, and −17.6 kcal mol^{-1} for **Mo-Pyr**, **W-Pyr**, and **Re-Pyr**, respectively), but associated with a relatively high energy transition state (16.0, 15.2, and 21.4 kcal mol^{-1} above separated ethene and hydride complex for **Mo-Pyr**, **W-Pyr**, and **Re-Pyr**, respectively). For the corresponding **M-Alk**, the process is less exoenergetic (−13.7, −16.4, and −11.0 kcal mol^{-1} for **Mo-Alk**, **W-Alk**, and **Re-Alk**, respectively) and associated with a lower energy transition state (14.8, 13.1, and 18.2 kcal mol^{-1} above separated ethene and hydride complex for **Mo-Alk**, **W-Alk**, and **Re-Alk**, respectively). Overall, complex **C** is always lower in energy than the SBP metallacycle by −7.2 to −10.7 kcal mol^{-1} and the transition state for ethene insertion in the M−H bond is always lower in energy than the transition state for β-H transfer. Thus, β-H transfer is the key step for the formation of side products and/or deactivation.

Subsequent Deactivation and Byproduct Formation Steps. From the ethyl complex **C**, three pathways are energetically accessible and involve H-transfer processes: β-H transfer from the ancillary alkyl ligand to the siloxy group leading to the cleavage of the M−O bond and thereby degrafting and α-H transfer from the ancillary alkyl ligand to the α- or γ-carbon of the 2-butenyl ligand leading to *E* 2-butene and 1-butene byproduct, respectively. The transition states for all these processes are lower in energy than the two previous steps. For the degrafting step, the reaction energy depends strongly on the metal and only slightly on the X ligand, the reaction is slightly exoenergetic for Re (−1.3 and −3.1 kcal mol^{-1} for **Re-Pyr** and **Re-Alk**, respectively), slightly endoenergetic for Mo (3.3 and 3.1 kcal mol^{-1} for **Mo-Pyr** and **Mo-Alk**, respectively) and highly endoenergetic for W (13.1 and 11.4 kcal mol^{-1} for **W-Pyr** and **W-Alk**, respectively). It is noteworthy that the transition state for formation of the ethyl complex **C** is typically higher in energy than this associated with its decomposition via degrafting for all systems at the exception of **W-Alk**. This suggests that **W-Alk** is less likely to be deactivated by degrafting.

Scheme 3

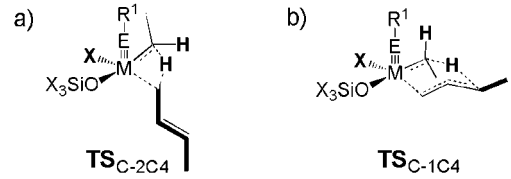

The reactions associated with the formation of butene byproduct and the regeneration of the catalyst are always highly exoenergetic (from −10 to −20 kcal mol^{-1}). The formation of 1-butene always goes via transition states of lower energy than this of 2-butene, most likely because of the preference for the less constrained six-member ring H-transfer transition state compared to a four-member ring H-transfer transition state (Scheme 3). In addition, the transition state for the formation of 1-butene and degrafting have similar energies, except for **Re-Pyr**, where degrafting is more favored.

Of the different elementary steps associated with deactivation and byproduct formation, these of β-H transfer and ethene insertion are the most disfavored by replacing the X alkyl ligand (**M-Alk**) by pyrrolyl (**M-Pyr**). On the other hand, the degrafting process depends on the metal center, rhenium complexes being the only ones with favorable degrafting thermodynamics.

Discussion

Overall, changing alkyl for pyrrolyl does not change the nature of the elementary steps associated with alkene metathesis, deactivation, and byproduct formation pathways. Remarkably, while it does not affect in a significant manner the energy profile of alkene metathesis, it has a profound influence on the energy of the transition state of the TBP−SPB interconversion as well as on the energy of the two steps that initiate the deactivation and byproduct formation, namely, the β-H transfer and the subsequent alkene insertion into the metal−hydride bond.

For alkene metathesis, coordination of the incoming alkene *cis* to the alkylidene ligand takes place *trans* to the stronger σ-donor X ligand versus siloxy; this also corresponds to the approach of the alkene to the most open of the two possible faces presenting the alkylidene ligand in the proper orientation. Moreover, the energy barrier for this step decreases with the increasing σ-donating ability of X; therefore, the replacement of an alkyl by a pyrrolyl ligand slightly increases the energy barrier for coordination in particular for Mo and W (<2 kcal mol^{-1}). In most cases, [2 + 2]-cycloaddition has a negligible energy barrier and leads to a TBP metallacycle. The energy of this metallacycle is only slightly stabilized by the pyrrolyl ligand in agreement with its weaker σ-donating ability.

From the TBP metallacyclobutane intermediate, the reaction can proceed either by productive metathesis (cycloreversion and decoordination) or by formation of the typically more stable SBP metallacyclobutane (resting state of the catalyst). The TBP−SBP interconversion takes place via a turnstile process, with an energy barrier significantly lower for **M-Pyr** than **M-Alk**. The energy of the transition states for TBP−SBP interconversion is always lower than these of cycloreversion for **M-Pyr** and similar for **M-Alk**. In contrast, from the SBP metallacyclobutane isomer, β-H transfer and ethene insertion

in the metal hydride bond initiating deactivation and byproduct formation have significantly higher transition states for **M-Pyr** than for **M-Alk** so that the transition state energies of these steps are higher than these of productive metathesis for **M-Pyr**, but not for **M-Alk**. Clearly, the pyrrolyl ligand disfavors the deactivation pathways. NBO analysis shows that this effect cannot be attributed to the pyrrolyl π-system. NBO analysis at the second order perturbation level shows that all M−H and M−C bonds are slightly strengthened by the presence of pyrrolyl, in agreement with a general shortening of the M−L distances. These effects are due to the more electronegative nature of N compared to C, which lowers, through an electrostatic effect, the energy of all orbitals with a metal contribution. In agreement with this analysis, the energy barriers for the β-H transfer and ethene insertion are also higher than for the **M-Alk** system when the pyrrolyl ligand is replaced by another amido group such as NMe_2 or an alkoxy group such as OMe (Figure 2). Reactions involving M−L cleavage such as β-H transfer and insertion are therefore expected to be disfavored by N- and O-based ligands. In contrast, alkene metathesis in which bonds are both broken and formed simultaneously at the metal is less affected.

These computational results are in full agreement with experimental data. First, both systems (X = alkyl and pyrrolyl), in particular for molybdenum, have similar potential energy surfaces. Therefore, the activity of the catalysts in terms of reaction rates (TOF) is expected to be similar (same order of magnitude). This is consistent with experimental data where similar initial rates have been observed for silica supported alkyl and pyrrolyl group 6 imido alkylidene complexes, [(≡SiO)M(═NAr)(═CHR^2)(X)] (M = Mo[12a,16] and W[13,17]). Second, TBP and SBP metallacyclobutanes are always close in energy (within 3 kcal mol^{-1}), and the TBP−SBP interconversion has accessible energy barriers especially for **M-Pyr**. Additionally, tungstacyclobutanes are calculated to be significantly more stable relative to separate reactants than their Mo and Re analogues. This is consistent with the recent observation of SBP (resting state) and TBP (intermediate) metallacyclobutanes for [(≡SiO)W(═NAr)(═CHR^2)(pyrrolyl)],[17] as well as with the fact that the corresponding Mo systems could not be observed under similar experimental conditions. Third, the two first steps of deactivation and byproduct formation (β-H transfer and ethene insertion) have transition states significantly higher in energy for **M-Pyr**, **M-NMe$_2$** and **M-OR**[31] than for **M-Alk** systems, which is consistent with the greater experimental stability and selectivity of [(≡SiO)M(═NAr)(═CHR^2)(pyrrolyl)], [(≡SiO)-M(═NAr)(═CHR^2)(NPh_2)], and [(≡SiO)M(═NAr)(═CHR^2)-(OR)] (R = alkoxy and fluoroalkoxy)[32] compared to [(≡SiO)-M(═NAr)(═CHR^2)(CH_2tBu)]. Fourth, W-based catalysts are calculated to be more stable metallacyclobutanes as well as less susceptible for deactivation (endoenergetic and higher activation barrier for degrafting), which is in agreement with their lower activity (TOF) and greater stability (higher TON).

Conclusion

In this study, we have shown that the concept of dissymmetry at the metal center is general and not limited to large differences of σ-donating ability between the X and Y ligands in [(X)M(ER^1)(═CHR^2)(Y)] alkene metathesis catalysts (Y = siloxy), since it applies for X = alkyl or pyrrolyl. This study also shows that the most open and reactive face of the tetrahedral [(X)M(ER^1)(═CHR^2)(Y)] catalysts with the proper alkylidene orientation is the face opposite to the stronger σ-donor X ligand, and therefore can be used as a rough guide for catalyst design. The greatest benefit of substituting the ancillary alkyl by a pyrrolyl ligand [(≡SiO)M(ER^1)(═CHR^2)(pyrrolyl)] is in fact *not to improve the efficiency of the catalytic cycle of alkene metathesis, but to shut down deactivation and byproduct formation pathways*. Remarkably, shutting down the deactivation pathway is not achieved by preventing the TBP−SBP interconversion, but by strongly disfavoring the decomposition of the SBP metallacycle via β-H transfer. The deactivation pathway is shown to be disfavored when the metal bound atom is more electronegative than carbon since other N- and O-based X ligands give similar results to pyrrolyl. Overall, dissymmetric catalysts with a pyrrolyl ancillary ligand are thus highly efficient because this ligand is optimal: (i) it is a better electron donor than the siloxy group, thus, favoring the metathesis pathway (dissymmetry at the metal center); and (ii) the nitrogen of the pyrrolyl ligand is more electronegative than the carbon of the alkyl group, thus, strengthening the M−L bonds and specifically disfavoring the decomposition of the metallacyclobutane intermediate via β-H transfer. Finally, while this study has been devoted to model the silica supported systems, hence the choice of Y = $OSiH_3$ (a model of siloxy group), the general aforementioned conclusions can be likely transposed to isoelectronic homogeneous systems based on X = pyrrolyl and Y = a bulky phenoxy ligand, which also display unprecedented activity and selectivity.[19,28] Delineating the differences between these homogeneous and heterogeneous catalysts (electronic, steric and dynamic effects), in particular the absence of formation of SBP metallacyclobutanes and decomposition via β-H transfer as well as the high *Z* selectivity for the former is currently underway.

Acknowledgment. We thank E. Clot (University Montpellier 2) and C. Landis (University of Wisconsin) for helpful discussions. The CESCA is acknowledged for a generous donation of computational time. X.S.-M. acknowledges the MICINN of Spain (Project CTQ2008-06381/BQU) and the Generalitat de Catalunya (Project SGR2009-638) for financial support as well as the MEC/MICINN for the Ramón y Cajal fellowship.

Supporting Information Available: Complete ref 21 and Tables S1−S9. Further comments on geometries and rotational barriers. Coordinates for all extrema with E and G (in a.u.). This material is available free of charge via the Internet at http://pubs.acs.org.

JA101597S

(31) Calculations were carried out for M = Mo, which are the only experimental systems reported.

(32) Rendón, N.; Berthoud, R.; Blanc, F.; Gajan, D.; Maishal, T.; Basset, J.-M.; Copéret, C.; Lesage, A.; Emsley, L.; Marinescu, S. C.; Singh, R.; Schrock, R. R. *Chem.—Eur. J.* **2009**, *15*, 5083–5089.